Original Article

Possible Effect of Intramural Botulinum Neurotoxin A Injection Versus Oral Resveratrol on Minimizing Hypertrophy, Fibrosis and Ultrastructural Changes of Detrusor Muscle Occurring Secondary to Partial Urethral Obstruction in Overactive Bladder Rat Model and Perspective on Their effect on TNFα, TGβ, PCNA, α-SMA and iNOS

Walaa Adel Abd el Moez Ahmed

Department of Anatomy and Embryology, Faculty of Medicine, Ain-Shams University, Egypt.

ABSTRACT

Introduction: The clinical condition of overactive bladder affects billions of individuals. The most prevalent cause is excessive detrusor activity. Patients whose symptoms are resistant to conventional treatment must be provided with novel treatment options.

Aim of the Work: Evaluation of effect of botulinum neurotoxin A injection compared to oral resveratrol on histopathological changes occurring secondary to partial urethral obstruction and evaluation of their effect on TNFα, TGβ, PCNA, α-SMA and iNOS.

Materials and Methods: 40 adult rats were included in the study. Group I (Sham group). GroupII: Partial urethral obstruction(PUO)-model was established and rats left for 6weeks. Group III: 10mg/kg resveratrol given by oral gavage for two weeks (from the sixth after PUO to the end of eighth week). Group IV: after PUO.50 ml botulinum neurotoxin A (BoNT-A) was injected in different walls of the bladder. Rats were left for another 2 weeks then sacrificed.

Results: Group II showed disrupted muscular bundles of muscularis propria. Muscle fibers appeared with extensive cytoplasmic vacuolations and abnormal shape of their nuclei. Masson's trichrome sections showed extensive collagen deposition in the bladder wall. Extensive reaction to PAS and deep staining of the muscle fibers. Transmission electron microscope showed irregular cell boundaries and bizarre shape of cell membrane. The myofibroblasts appeared extensively invading the intermuscular septa. Some muscle fibers appeared degenerated with extensive infiltrate by mast cells and fibroblasts. Besides, extremely dilated nerve endings with clustered degenerated bodies at their lower ends. Congested, dilated blood vessels could also be detected. There was marked increase in the oxidative stress markers and proinflammatory cytokines. All previous Changes greatly improved in groups III and IV and the best results were observed in group IV.

Conclusion: Resveratrol and botulinum neurotoxin are new lines of management to patients suffering from refractory symptoms of overactive bladder.

Received: 20 May 2023, **Accepted:** 13July 2023

Key Words: Botulinum toxin; detrusor muscle; resveratrol.

Corresponding Author: Walaa Adel Abd el Moez Ahmed, MD, Department of Anatomy and Embryology, Faculty of Medicine, Ain-Shams University, Egypt. **Tel.** +2 012 0118 3689, **E-mail:** Walaa_adel@med.asu.edu.eg

ISSN: 1110-0559, Vol. 47, No. 3

INTRODUCTION

Damage to detrusor muscles caused by obstruction of the bladder outlet impacts billions of people worldwide, particularly men with benign prostatic hyperplasia. In addition, histological and functional alterations of the detrusor muscle may be a possible contributor in the pathogenesis of overactive bladder (OAB)[17]. There have been numerous proposed interventions for OAB, including medical and surgical options. Antimuscarinics agents are a popular treatment option for OAB symptoms. Nevertheless, their efficacy and adverse effects typically result in low compliance[12]. Surgical options, on the other hand, are typically reserved for resistant and complicated cases. New perspectives and treatment modalities are still rendered and regarded as a focus of current research.

Resveratrol is a creative molecule that has captured the attention of scientists. It consists of pine tree, grape, mulberry, and pistachio extracts. Moreover, resveratrol receives significant interest from the general public, research community and natural medicine field[19]. In addition, resveratrol's anti-inflammatory and anti-oxidant properties have been demonstrated in previous experimental and clinical studies[23]. The capacity of resveratrol to reduce the biochemical and histological changes associated with OAB requires extensive additional research.

DOI: 10.21608/ejh.2023.212302.1897

Botulinum Neurotoxin-A is one of the most potent toxins in the world. It can provide a wide range of therapeutic benefits. It is known with its ability to inhibit the release of acetylcholine at the neuromuscular junction, thereby inhibiting the contraction of smooth muscle[6]. Moreover, it has been widely utilized for multiple purposes such as hyperhidrosis and other noninvasive cosmetic facial procedures[4]. Decreased detrusor muscle contractility by intramural botulinum neurotoxin may significantly reduce OAB symptoms and enhance the quality of life of the patient.

AIM OF WORK

The aim of the current investigation was evaluating the effect of botulinum neurotoxin A injection in comparison with oral resveratrol on structural changes occurring secondary to partial urethral obstruction in an overactive bladder created rat model. Rendering a new perspective about their effect on tumor necrosis factor alpha (TNFα), transforming growth factor beta (TGβ), proliferating cell nuclear antigen (PCNA), alpha smooth muscle actin (α-SMA) and inducible nitric oxide synthase (iNOS).

MATERIAL AND METHODS

Ethical approval

The study was approved by the Ethical Committee of Ain Shams University, with approval number FWA 000017585.Methods of the current investigation were utilized in accordance with (CARE) guidelines. The local Medical School- Ain Shams University Research Ethics Committee

Experimental drugs

Botulinum Toxin- A (Botox®): Botulinum Toxin - A Injection 100IU.The drug manufactured in Life cura Pharma, Chembur, Mumbai, Maharashtra. Purchased from IN CLINC, Cairo, Egypt.

Resveratrol (Resveratrol®): Resveratrol 100mg crystalline powder. The drug was purchased from Sigma Company, Nasr city, Cairo, Egypt.

Experimental design & Procedures

Four groups of 40 adult male wistar albino rats weighing between 150 and 200 g were created. They were confined in 30x35cm enclosures made of stainless steel that contained two rats per cage. The investigation excluded rats with a disease, those that had been used in previous experiments, those that had difficulty walking, or those with poor fur. Rats were exposed to an environment and ventilation that were suitable.

Partial bladder outlet obstruction rat model (PUO)

Surgery was performed in Faculty of Medicine Ain Shams Research Institute (MASRI). PUO was created under anesthesia with ketamine (100 mg/kg, intraperitoneal) + chlorpromazine (30 mg/kg, intraperitoneal). A 5-cm midline vertical incision on the lower part of abdominal wall was made to gain access to urinary bladder and urethra. The sterile metal bar of 19F urethral catheter was placed on the urethral orifice and a non-absorbable 4–0 polypropylene suture was passed under the urethra to include the urethra and a catheter together. Finally, a tie was placed around the urethra and the catheter. As soon as the suture was secured, the bar was removed, leaving the urethra partially obstructed[24].

Experimental design & procedures

40 adult male wistar albino rats were included in the study and were divided into four groups/ten rats each.

Group I (Sham group): the same procedure was performed as mentioned before. The skin, the peritoneum and the abdominal wall were opened and re-closed but without obstruction of the urethra. Rats were left for 8 weeks.

GroupII (PUO-operated group): operation was done as described previously under complete aseptic condition then, rats were left for 6weeks duration[24].

Group III (Resveratrol - treated group): rats underwent the PUO surgery as group II+10mg/kg/d resveratrol dissolved in normal saline given by oral gavage for two weeks (from the sixth week after PUO to the end of eighth week of the experiment)[25].

Group IV (PUO + BoNT-A -treated group): Six weeks after PUO, utilizing sterile aseptic techniques. Ketamine (100 mg/kg, ip) and chlorpromazine (30 mg/kg, ip) were used to induce anesthesia in rats. A midline abdominal incision to re-expose the urinary bladder. In five equal doses; each one 10 IU. A total 50 ml of BoNT-A was instilled into the anterior, posterior, left, and right lateral walls and dome of the bladder. The epidermis and abdominal wall were then closed in two layers. The abdominal wall muscles were sutured by vicryl 3-0 and the skin sutured by proline 4-0. Two more weeks passed before the rats were sacrificed[14].

Tissue sampling

At the end of the experimental period, rats were rendered unconscious with an intraperitoneal injection of ketamine (90 mg/kg), xylazine (15 mg/kg) and afterwards sacrificed. Urinary bladder samples were dissected and collected for histopathological and immunohistochemical investigations.

Histological and immunohistochemical techniques

For Light microscopic study

Urinary bladder samples were dissected to transverse sections, fixated for ten days in 10% neutral formalin and processed into paraffin blocks. Paraffin blocks were cut to a thickness of 5 to 7 µm and stained with H&E, Masson's trichrome, and Periodic Acid-Schiff stain (PAS)[2]. Other specimens were rinsed for two hours in phosphate buffer, and then the specimens were prepared for semithin sections. Semithin sections of one-micron thickness were cut using a

glass knife. They were stained with a 1% concentration of toluidine blue. The stained sections were investigated using an Olympus light microscope equipped with an automatic photomicrographic camera system. Kodak ASA400 film was utilized for the color prints[13].

For Immunohistochemistry

Immunohistochemical examination was conducted on paraffin-embedded tissues using the antibodies Proliferating Cell Nuclear Antigen (PCNA) and alpha smooth muscle actin (α-SMA). The paraffin sections were placed on slides that were coated with Poly-L-Lysine. After deparaffinization, phosphate buffered saline (PBS) containing 3% hydrogen peroxide; the slides were incubated for 5 minutes to inhibit endogenous peroxidase. The secondary antibodies used were Envision + Horseradish peroxidase system (HRP) antirabbit for α-SMA and PCNA. Diaminobenzidine was utilized as the chromogen. As a final counterstain, haematoxylin was applied[1].

For Electron Microscopy

Following the standard protocol for preparing samples of the urinary bladder for transmission electron microscopy. Urinary bladder tissue fragments were rinsed in phosphate- buffered saline two hours after fixation in 2.5% phosphate- buffered glutaraldehyde at 4°C. Urinary bladder specimens were then post fixed for one hour at 4°C in 1% phosphate buffer osmium tetroxide. The urinary bladder samples were then dehydrated in ascending concentrations of alcohol, submerged in propylene oxide, and encapsulated with an epoxy resin mixture. Semithin sections were examined by light microscope L/M to identify the appropriate regions. Contrast agents; uranyl acetate and lead citrate were used to investigate ultrathin sections (80-90nm thick)[13]. The slices were viewed with a transmission electron microscope (TEM) ("Jeol" E.M.-100 CX11; Japan) at electron microscopy unit Faculty of Science; Ain Shams University.

For Biochemical analysis

Blood samples were allowed to coagulate for ten minutes prior to being centrifuged at 4,000 revolutions per minute. To evaluate the inflammatory condition, serum levels of Tumor Necrosis Factor alpha (TNF-α) and Transforming Growth Factor Beta (TGFβ) were measured using ELISA kits (E-EL-R0015, Elabscience Biotechnology, USA) and (E-EL-R1015, Elabscience Biotechnology, USA), respectively. ELISA assays kit number E-BC-K025-S (Elabscience Biotechnology, USA) and E-BC-K020 (Elabscience Biotechnology, USA) were used to measure oxidative stress markers such as inducible nitric oxide synthase (iNOS) and Malonaldhyde dehydrogenase (MDA) to determine the oxidative stress state.

Histomorphometric results

Quantitative Image Analysis

Using image analyzer, the measurements were performed in the Histology and Cell Biology Department of the Ain Shams University Faculty of Medicine. Calculating the area% of immunological staining required use of seven fields from seven independent serial sections from seven animals from each group. The image analyzer was initially automatically calibrated to convert the measurement units (pixels) generated by image analyzer application into actual micrometer units. Before measuring the positively reacting PCNA & α-SMA immunostained patches in each field using the standard measurement frame, a blue binary pigment was applied to the positively reacting PCNA & α-SMA immunostained patches in each field. PCNA & α-SMA expression was quantified by comparing the proportion of positively stained regions to the total tissue area of the urinary bladder.

Statistical analysis

The collected data were presented as mean ± SD. Version 23 of SPSS was used for data analysis. The significance of differences between groups was determined utilizing one-way analysis of variance (ANOVA) and the Bonferroni post-hoc test. The result was deemed statistically significant when the *P-value* was less than 0.05.

RESULTS

A metal bar with a 0.91-mm diameter of urethral catheter inserted on the urethral orifice (Figure 1A). Then, a non-absorbable 4–0 polypropylene suture is passed under the urethra to include the urethra and a catheter together (Figure 1B). Moreover; a tie is placed around the urethra and the catheter. An intramural botulinum toxin injected in fundus and walls of the bladder (Figures 1C,D,E). Furthermore; the abdominal incision sutured in double layers (Figures 1F,G) showing extracted dissected urinary bladder from different groups. There is a marked enlargement in the size of urinary bladder clearly shown in groups II and III.

Histopathological results

Examining sections of the control group (I) stained with H&E and toluidine blue under light microscope revealed normal thickness of the muscularis propria and intermuscular septa. It appears consisting of inner longitudinal, middle circular and outer longitudinal muscle layers and interlacing with each other (Figures 2A, 4A). Group II showing disrupted muscular bundles of the muscularis propria with complete loss of their normal shape and arrangement and relative increase in thickness of the muscularis propria (Figures 2B,4B). On other hand, obvious restoration of normal shape, arrangement and even thickness of the muscular bundles of muscularis propria was clearly observed in groups III and IV (Figures 2C,4C,2D,4D).

Furthermore, with higher magnification of the previous sections; the muscle fibers appeared with well-defined cell boundaries and normal thickness of intermuscular septa. The elongated and rounded nuclei of the longitudinal and circular muscle fibers were clearly identified in group (I) (Figure 3A). In group II, the muscle fibers appeared with ill-defined borders and extensive cytoplasmic vacuolations. Besides, pale staining and abnormal shape of their nuclei (Figures 3B,4B). In contrast, the muscle fibers of the muscularis propria in group III appeared with dark staining of their nuclei and moderate thickness of intermuscular septa but with persistence of abnormal shape of the nuclei and some cytoplasmic vacuolations (Figures 3C,4C). In contrast, group IV showed apparent normal thickness of the septa, the muscular fibers appeared with normal shape of the nuclei with no cytoplasmic vacuolations (Figures 3D,4D).

Masson's trichrome sections revealed normal collagen deposition in the bladder wall and in-between the muscular bundles of the muscularis propria (MP) in group (I) (Figure 5A). Moreover, group II showed extensive collagen deposition in all layers of the bladder wall especially in the muscularis propria (Figure 5B). In contrast to the mild to moderate collagen deposition which was clearly detected in groups III and IV(Figures 5C,D).

In addition, PAS stained sections of group I showed mild reaction, the muscle bundles appeared with mild staining (Figure 6A). GroupII showed extensive reaction to PAS with deep staining of the muscle fibers (Figure 6B). In contrast to the mild to moderate reaction to PAS which was clearly detected in groups IV and III (Figures 6C,D).

Immunohistochemical Results

Group I showed negative reaction to PCNA in the muscularis propria (Figure 7A). Extensive reaction to PCNA was clearly detected in the muscularis propria in group II (Figure 7B). In addition, moderate reaction to PCNA was detected in group III (Figure 7C). Finally, a mild reaction was clearly observed in group IV(Figure 7D).

Immunohistochemical results to α-SMA stained sections showed negative reaction in both groups I&IV (Figures 8A,D). In contrast to the intense positive reaction which was detected as granular brownish staining in-between the muscular bundles of the muscularis propria (Figure 8B). Finally, moderate reaction to α-SMA was observed in group III (Figure 8C).

Examination of group I sections by transmission electron microscope revealed the circular and longitudinal muscle fibers with well-defined cell boundaries and normal thickness of intermuscular septa (Figures 9A,B). In addition, the normal appearance of the nerve terminals at the neuromuscular junctions (Figure 10A). GroupII showed irregular cell boundaries with peripheral edema (oak leaf pattern) and outward bulging of cell membrane. The myofibroblasts appeared extensively invading the intermuscular septa. Moreover, in some areas the muscle fibers appeared degenerated with extensive cytoplasmic vacuolations and extensive inflammatory cell infiltrate. Both mast cells and fibroblasts were clearly observed. Other areas appeared with extensive collagen deposition in the muscularis propria (MP) (Figures 9C,D,E,F). Furthermore, the extremely dilated nerve endings with clustered degenerated bodies at their lower ends and extremely dilated congested blood vessels could also be detected (Figures 10B,C,D).

Group III showed moderate collagen deposition in between the muscular bundles of muscularis propria, some cytoplasmic vacuolations still detected with mononuclear inflammatory cell infiltrate (Figures G,H,I). Finally, group IV showed apparent normal appearance of the circular and longitudinal muscle bundles with normal thickness of the intermuscular septa but with few detected mononuclear inflammatory cells (Figures 9 j,k,L). Apparent restoration of normal nerve terminals at the neuromuscular junctions and improved condition of the blood vessel wall in groups III and IV (Figures 10 E,F,G,H).

Histomorphometric and statistical results

Area %of PCNA in muscularis propria of urinary bladder (Table 1, Histogram 1)

Compared to the other groups, group II showed significant increase in the area% stained with PCNA based on the data presented in table1. Group III showed significant decrease relative to group II, but significant increase relative to I and IV. Group IV demonstrated significant decrease relative to II and III, but significant increase relative to I.

Area % of α-SMA in the muscularis propria of urinary bladder (Table 2, Histogram 2)

Compared to other groups, group II showed highly significant increase in the mean area % of α-SMA based on the data presented in table 2. Group III showed highly significant decrease relative to II, but a highly significant increase relative to I. Group IV showed highly significant decrease relative to II and III, but no significant decrease relative to I.

Area % of collagen distribution in muscularis propria of urinary bladder (Table 3, Histogram 3)

Compared to other groups, group II showed significant increase in the mean area % of collagen deposition based on the data presented in table 3. Group III showed significant decrease relative to II, but significant increase relative to groups I and IV. Group IV showed a significant decrease relative to II and III, but a significant increase relative to I.

Statistical results of TGβ levels in rat serum (Table 4, Histogram 4)

Compared to other groups, group II showed highly significant increase in the serum level of TGβ relative to other groups based on the data presented in table 4. Group III showed highly significant decrease relative to II. Group

IV demonstrated highly significant decrease relative to II, but no statistically significant decrease relative to I and III.

Statistical results of TNF-α levels in rat serum (Table 4, Histogram 5)

Compared to other groups, group II showed highly significant increase in the serum level of TNF-α based on the data presented in table 4. Group III showed highly significant decrease relative to II, but significant increase relative to I. Group IV showed significant decrease relative to II. No significant decrease relative to group III and no significant increase relative to I.

Statistical results of iNOS levels in rat serum (Table 4, Histogram 6)

Compared to other groups, group II showed highly significant increase in the serum level of SOD with based on the data presented in table 4. Group III showed highly significant decrease relative to II, but a highly significant increase relative to I and IV. Group IV showed significant decrease relative to II and III, but no significant decrease relative to I.

Statistical results of MDA levels in rat serum (Table 4, Histogram 7)

Compared to other groups, group II showed highly significant increase in the serum level of MDA based on the data presented in table 4. Group III showed highly significant decrease relative to group II, but highly significant increase relative to I and IV. Group IV showed high significant decrease relative to I, II and III.

Measurements of thickness in µm of the muscularis propria among different groups (Table 5, Histogram 8)

Compared to other groups, group II showed highly significant increase in the thickness of the muscularis propria based on the data presented in table 5. Group III showed a highly significant decrease relative to group II, but shows no statistical difference relative to I and IV. Group IV showed significant decrease relative to group II and no statistical difference relative to I and III.

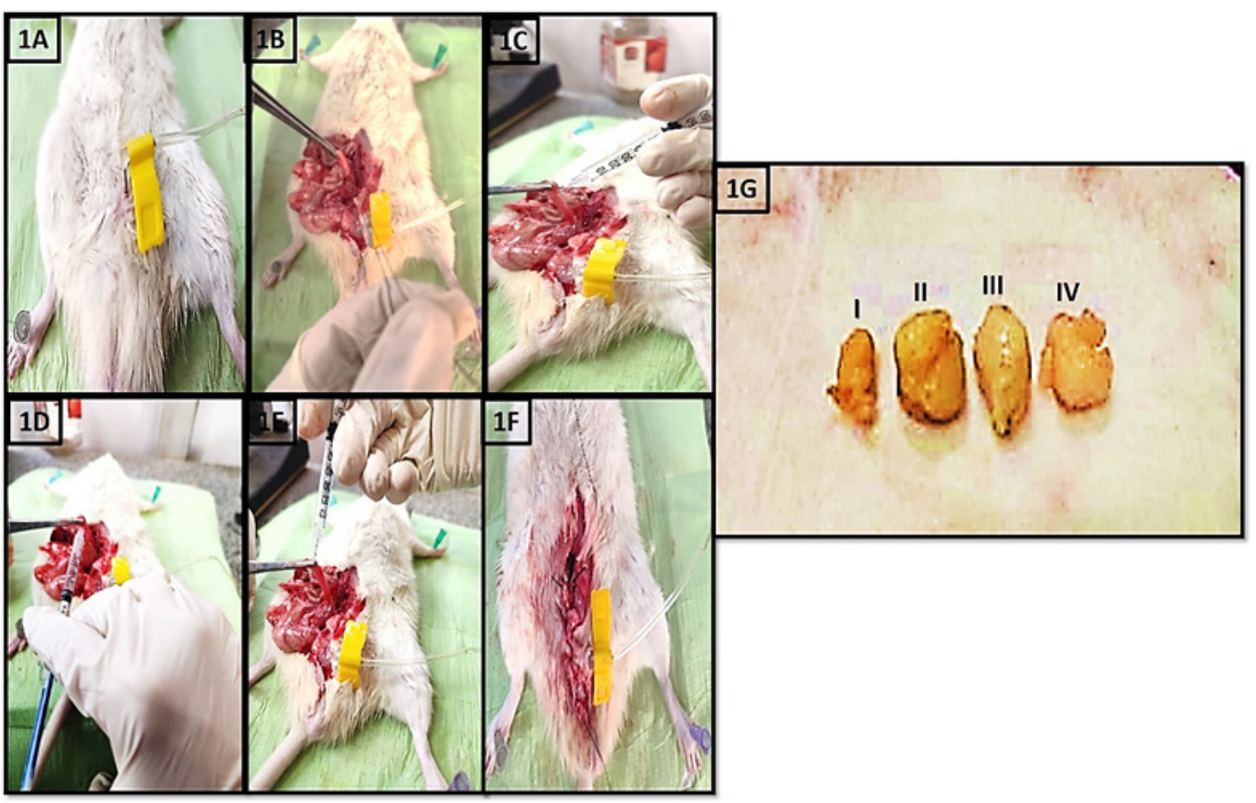

Fig.1: A: photomicrograph showing a sterile metal bar with a 0.91-mm diameter of urethral catheter inserted on the urethral orifice.Fig.1B: showing a non-absorbable 4–0 polypropylene suture is passed under the urethra to include the urethra and a catheter together. A tie is placed around the urethra and the catheter. Figs.:1C, D, E: showing intramural botulinum toxin injection in the fundus of urinary bladder. Fig.1F: showing the abdominal incision sutured in double layers.Fig.1G: showing extracted dissected urinary bladder from different groups. Note, marked enlargement in the size of urinary bladder in groups II and III.

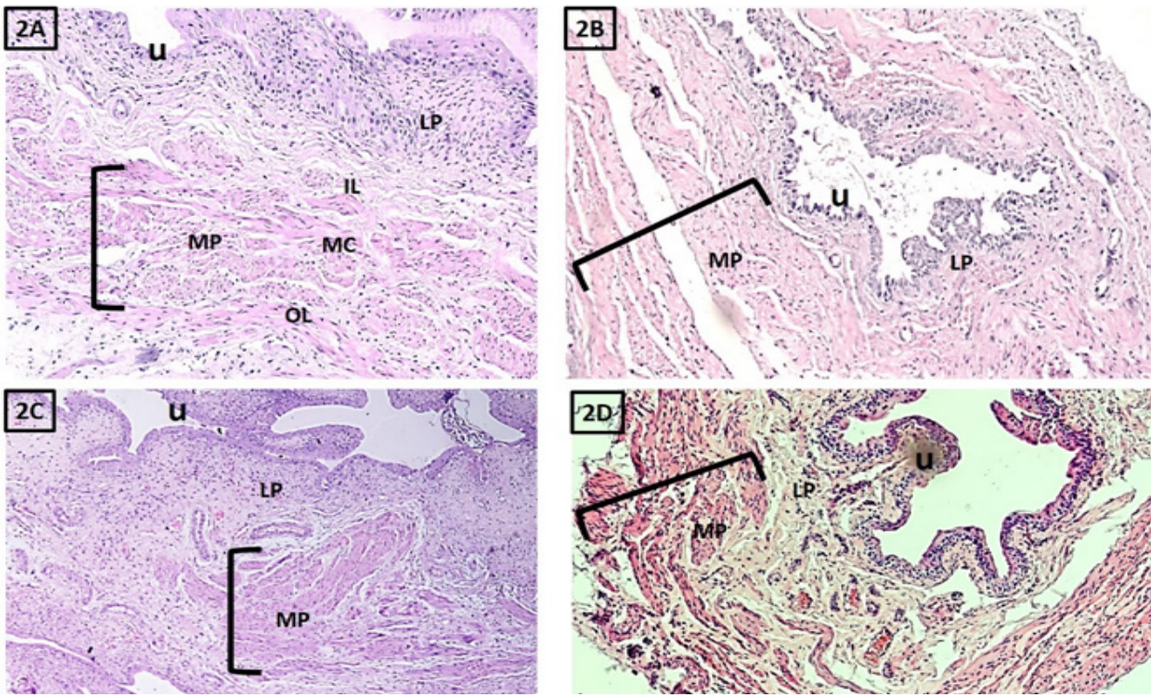

Fig. 2: A: photomicrograph of section in urinary bladder wall showing different layers of bladder wall (U) urothelium, (LP) lamina propria and (MP) muscularis propria. Normal thickness and normal arrangement of muscular bundles of the muscularis propria(MP). It appeared consisting of inner longitudinal(IL), middle circular(MC) and outer longitudinal bundles(OL). Fig.2B: showing marked increase in the thickness of detrusor muscle(MP) with complete loss of their normal arrangement.Fig.2C: showing moderate restoration of normal thickness of detrusor muscle(MP) but with complete loss of their normal arrangement. Fig. 2D: showing an obvious restoration of normal shape, thickness and arrangement of the muscularis propria(MP)(H&Ex100).

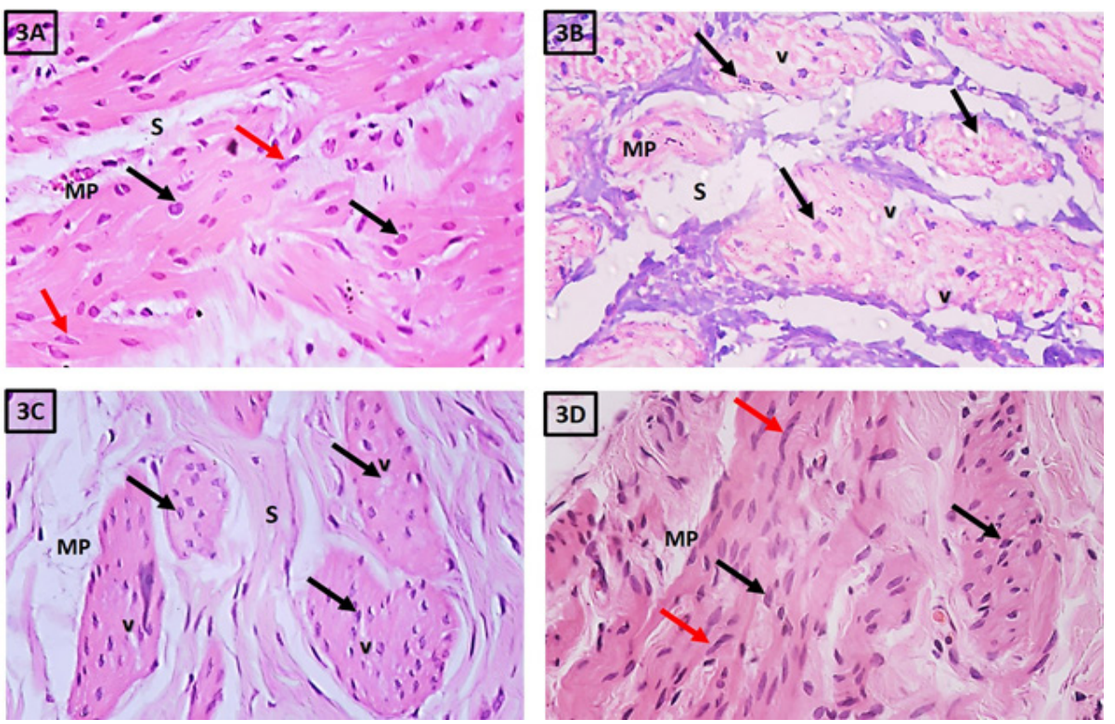

Fig. 3: A: photomicrograph of a section in the urinary bladder wall showing the muscularis propria (MP) consisting of longitudinal (red arrows) and circular (black arrows) muscle fibers with well-defined borders, dark staining of their nuclei and normal thickness of intermuscular septa (S). Fig.3B: showing the muscle fibers with ill-defined cell borders, pale staining and obvious change in the shape of their nuclei with extensive cytoplasmic vacuolations (v). Fig.3C: showing moderate restoration of cell boundaries, thickness of intermuscular septa(s) but with persistence of abnormal shape of the nuclei (black arrows) and cytoplasmic vacuolations(V). Fig.3D: showing the elongated (red arrows) and circular nuclei (black arrows) of muscle bundles and normal thickness of intermuscular septa(S) with no cytoplasmic vacuolations(H&Ex400).

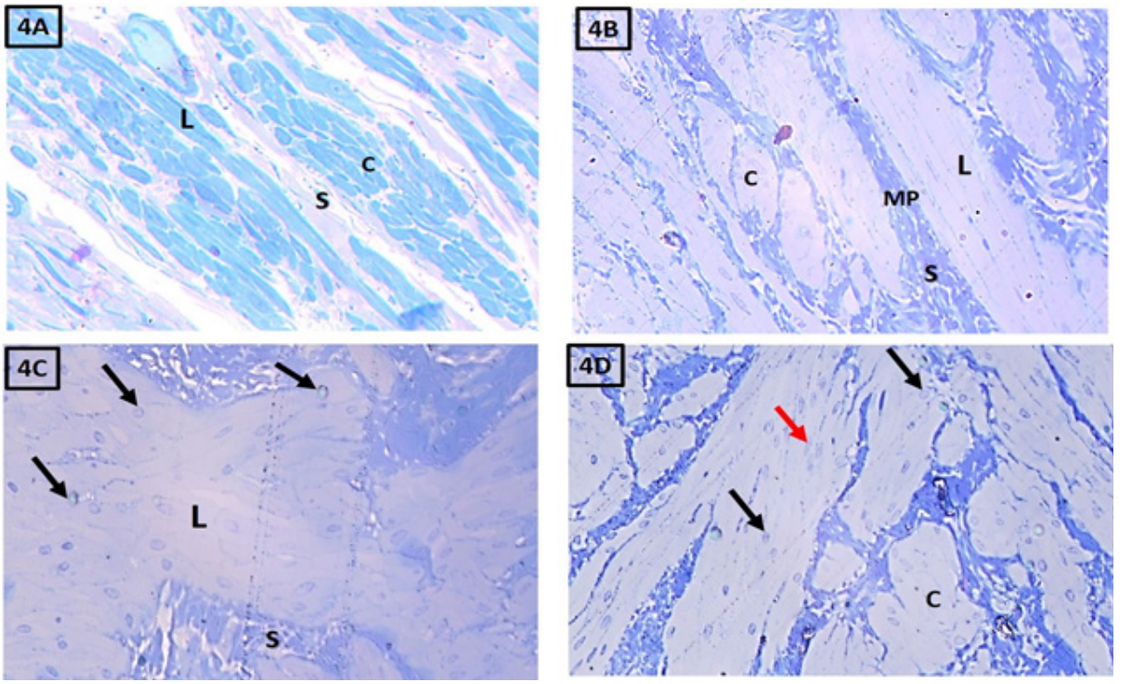

Fig. 4: A: photomicrograph of a section in the urinary bladder wall showing the muscularis propria (MP) consisting of longitudinal(L) and circular (C) muscle fibers with well-defined borders and normal thickness of intermuscular septa (S). Fig.4B: showing the muscle fibers with ill-defined cell borders, pale staining and hard detection their nuclei. Fig.4C: showing moderate restoration of normal cell boundaries and moderate thickness of intermuscular septa(s) but with persistence of abnormal shape of the nuclei (black arrows). Fig.4D: showing the elongated (red arrows) and circular nuclei (black arrows) of muscle bundles, well defined cell borders, normal thickness of intermuscular septa(S) with no cytoplasmic vacuolations. (Toluidine bluex400)

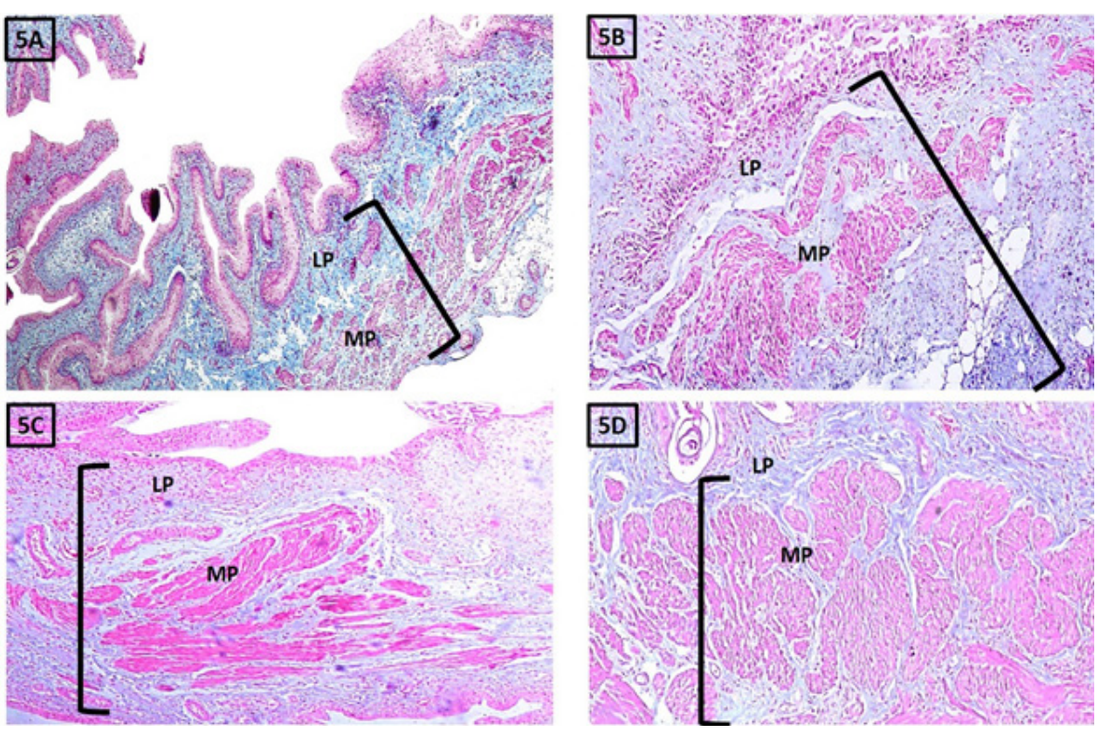

Fig. 5: A: photomicrograph of a section in the urinary bladder wall showing normal collagen deposition in the bladder wall, in both the lamina propria (LP) and the muscularis propria(MP). Fig.5B: showing extensive collagen deposition in all layers of the bladder wall especially in the muscularis propria(MP) with marked increase in the thickness of the bladder wall.Fig.5C: showing moderate collagen deposition in the muscularis propria(MP) and moderate increase in the bladder wall.Fig.5D: showing mild collagen deposition in the bladder wall. (Masson's trichrome x100)

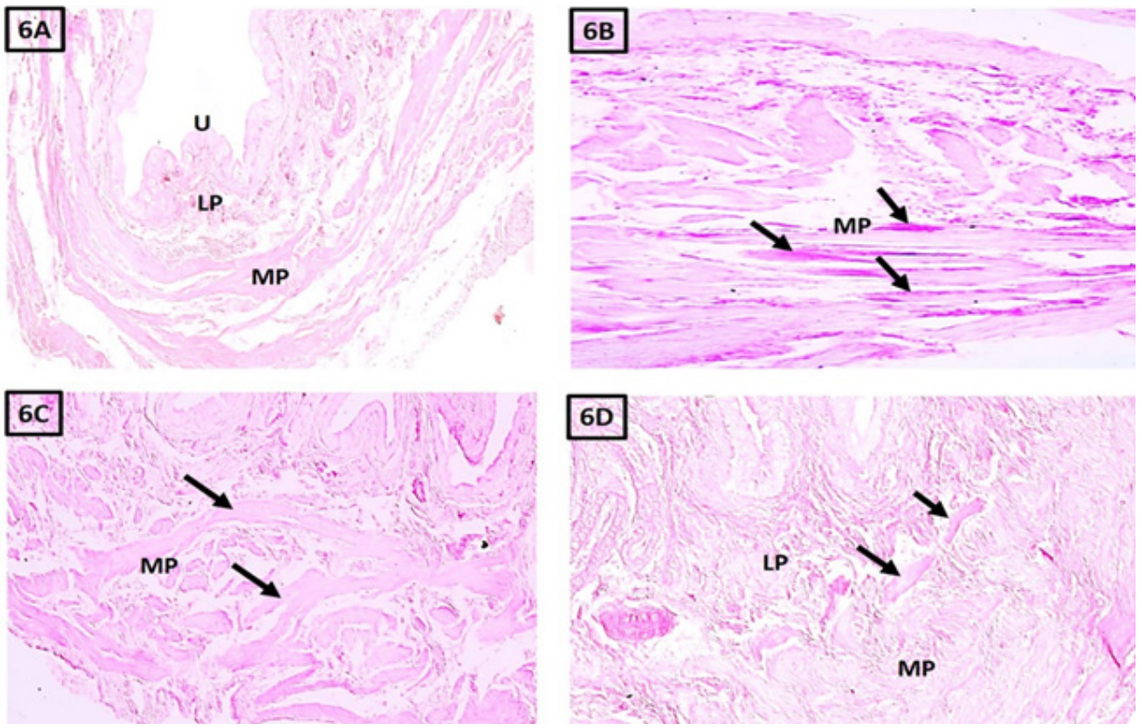

Fig. 6: A: photomicrograph of a section in the urinary bladder wall showing urothelium(U), lamina propria (LP) and muscularis propria (MP); there is negative reaction to PAS with pale staining of the muscular fibers of detrusor muscle.Fig.6B: showing intense positive reaction to PAS the muscular bundles of detrusor muscles appeared deeply stained.Fig.6C: showing moderate reaction to PAS in the muscularis propria(MP). Fig.6D: showing negative reaction to PAS in the muscularis propria(MP) (black arrows).(PASx100)

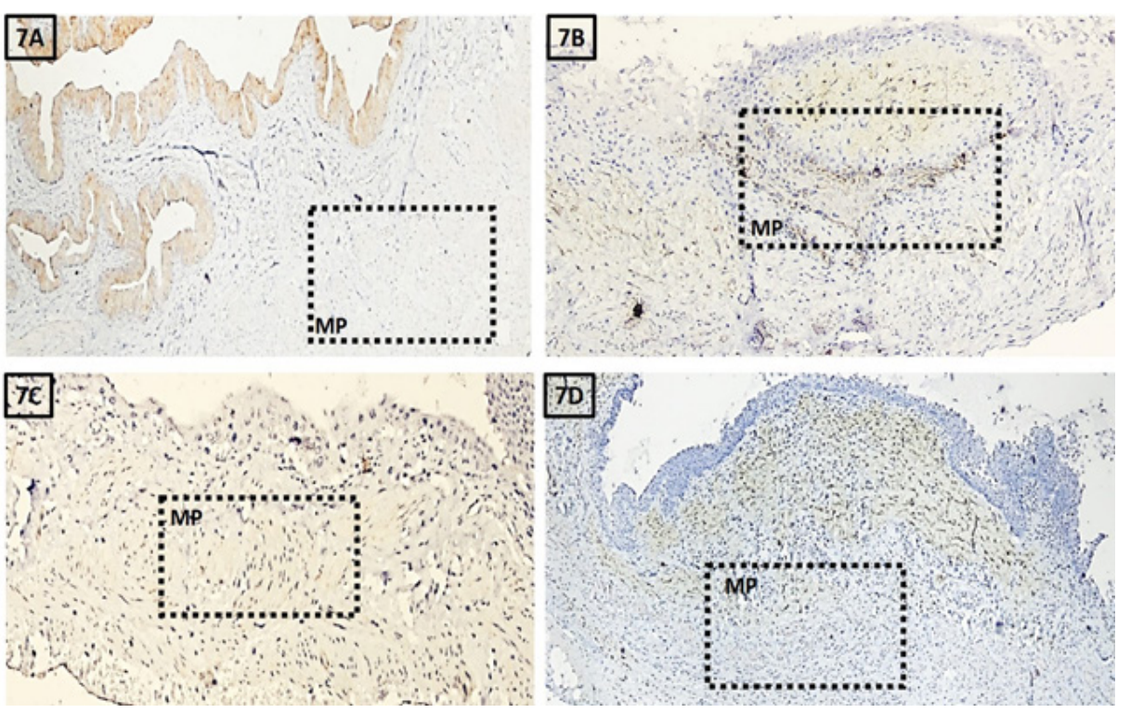

Fig. 7: A: photomicrograph of a section in the urinary bladder wall showing negative immune reaction to PCNA in the muscularis propria(MP) (the inset). Fig.7B: showing intense immune reaction to PCNA in the muscularis propria, the reaction appeared as intense brownish cytoplasmic staining of the fibers of detrusor muscle (the inset). Fig.7C: showing moderate immune reaction to PCNA in the muscularis propria(MP) (the inset). Fig.7D: showing mild immune reaction to PCNA in the muscularis propria(MP) (the inset).x100

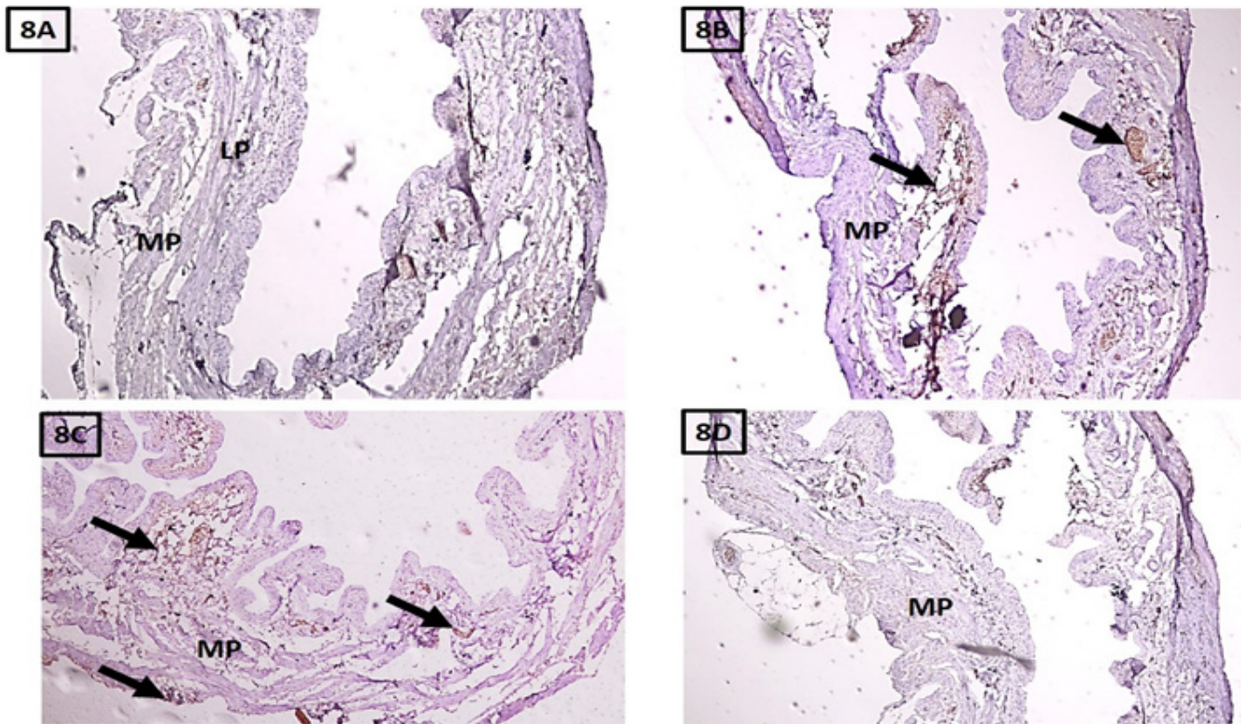

Fig. 8: A: photomicrograph of a section in the urinary bladder wall showing lamina propria (LP) and muscularis propria (MP); there is negative immune reaction to α-SMA in the muscularis propria(MP). Fig.8B: showing intense immune reaction to α-SMA appeared as granular brownish staining in between muscular bundles of the muscularis propria(MP) (black arrows). Fig.8C: Showing moderate immune reaction to α-SMA in the muscularis propria (black arrows). Fig.8D: showing negative immune reaction to α-SMA in the muscularis propria(MP).x100

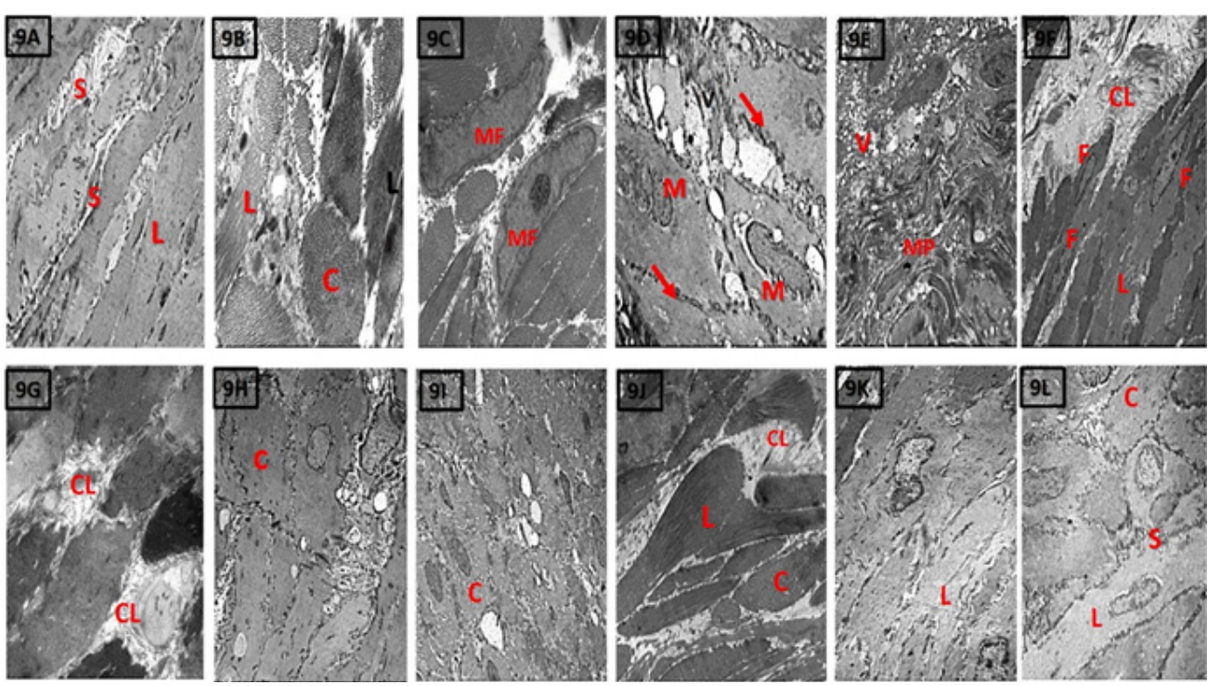

Figs. 9: A,B: photomicrograph of a section in the urinary bladder wall showing the circular(c) and longitudinal(L)muscle fibers with well-defined cell boundaries and normal thickness of intermuscular septa(S).Fig.9C,D,E,F: showing irregular cell boundaries with peripheral edema(oak leaf pattern) and outward bulging of cell membrane(red arrows), the myofibroblasts invading the intermuscular septa, in some areas the muscle fibers appeared degenerated with extensive cytoplasmic vacuolations (V), macrophage (M) and fibroblasts (F) infiltrating the detrusor muscle fibers with extensive collagen(CL) deposition in the muscularis propria(MP).Figs.9 G, H,I: showing moderate collagen(CL) deposition in between the muscular bundles of muscularis propria, some cytoplasmic vacuolations still detected. Figs9 j, k, L: showing normally appearing circular and longitudinal muscle bundles with normal thickness of intermuscular septa(s). Lead acetate x1200,3000, 2500,2000,1200,1200,2500,1000,1200,1000,1000,1000 respectively)

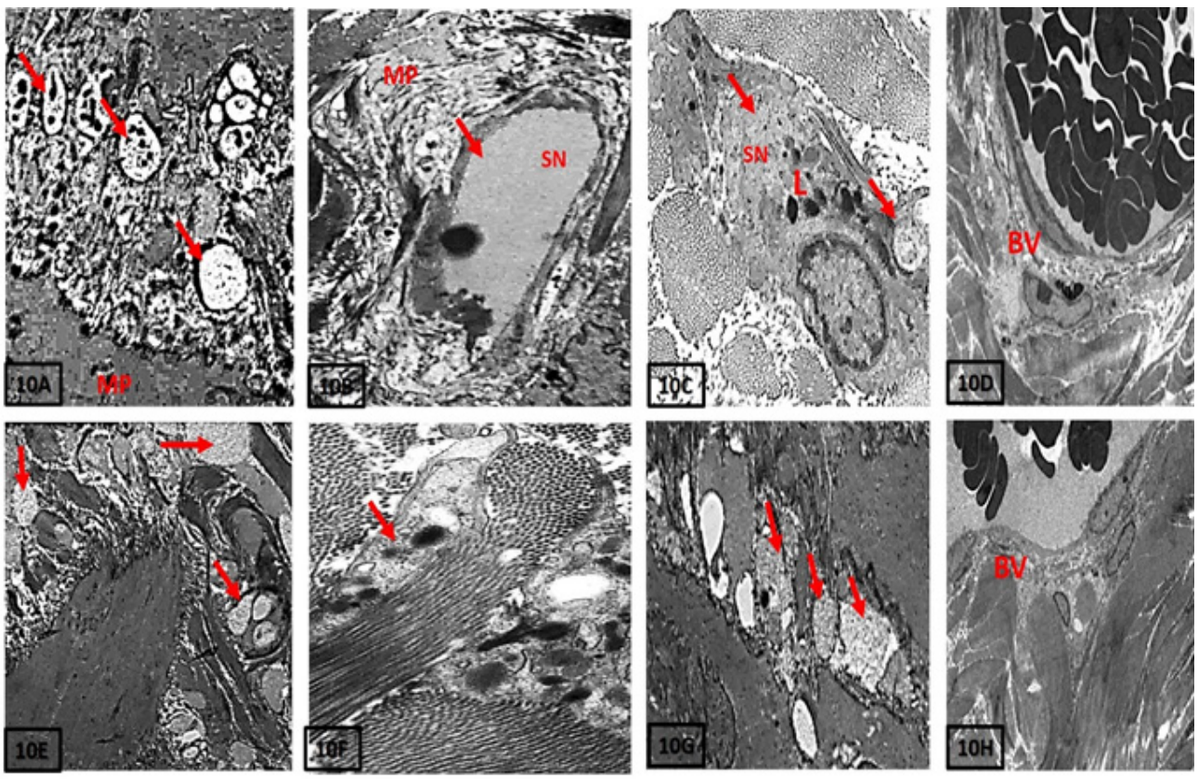

Fig. 10: A: photomicrograph of a section in the urinary bladder wall showing the nerve endings forming junctions with muscle cells in the muscularis propria(MP); the nerve ending at the neuromuscular junction almost normal in appearance (red arrows). Figs.10(B&C&D) an extremely swollen nerve(SN) ending with clustered vesicles and degenerated bodies at its lower end (red arrow) with lysosomal bodies (L), congested dilated blood vessel(BV). Figs.10(E&F&G): showing apparent restoration to the normal appearance of the nerve terminals (red arrows), decreased congestion, improved blood vessel wall condition(BV). (Lead acetatex5000,5000,4000,2500,3000,3000,5000,2500 respectively)

Table 1: illustrates area % of PCNA immunoreaction in the muscularis propria

Mean area % of PCNA	Control group	PUO group	Resveratrol	Botulinum neurotoxin A	Test value	*P-value*	Sig.
	No. = 7	No. = 7	No. = 7	No. = 7			
Mean ± SD	0.65 ± 0.10	12.36 ± 1.14	4.49 ± 0.88	1.72 ± 0.24	364.72•	<0.001	HS
Range	0.54 – 0.81	10.95 – 14.32	3.47 – 5.64	1.44 – 2.04			
			Post Hoc analysis				
P1		P2	P3	P4	P5	P6	
<0.001		<0.001	0.011	<0.001	<0.001	<0.001	

P-value > 0.05: Non significant; *P-value* < 0.05: Significant; *P-value* < 0.01: Highly significant •: One Way ANOVA test. P1: Control Vs PUO group; P2: Control Vs resveratrol group; P3: Control Vs botulinum neurotoxin A; P4: PUO Vs resveratrol; P5: PUO Vs botulinum neurotoxin A; P6: Resveratrol Vs botulinum neurotoxin A

Table 2: Mean area % of α-SMA in the muscularis propria of urinary bladder

α-SMA	Group I (control)	Group II (BOO-Created)	Group III (Resveratrol treated)	Group IV (Botulinum toxin -treated)	Test value	*P-value*	Sig.
	No. = 7	No. = 7	No. = 7	No. = 7			
Mean ± SD	0.40 ± 0.16	5.66 ± 0.91	2.51 ± 0.36	0.91 ± 0.07	158.647•	0.000	HS
Range	0.16 – 0.66	4.03 – 6.65	2.07 – 2.98	0.79 – 0.99			
			Post Hoc analysis by LSD				
P1		P2	P3	P4	P5	P6	
<0.001		<0.001	0.064	<0.001	<0.001	<0.001	

P-value > 0.05: Non significant; *P-value* < 0.05: Significant; *P-value* < 0.01: Highly significant•: One Way ANOVA test P1: group I Vs group II; P2: group I Vs group III; P3: Group I Vs group IV; P4: Group II Vs group III; P5: Group II Vs group IV; P6: Group III Vs group IV.

Table 3: Mean area % of collagen distribution in the muscularis propria of urinary bladder

Collagen deposition in muscularis propria	Group I (control)	Group II (BOO-Created)	Group III (Resveratrol treated)	Group IV (Botulinum toxin -treated)	Test value	*P-value*	Sig.
	No. = 7	No. = 7	No. = 7	No. = 7			
Mean ± SD	1.75 ± 0.22	13.79 ± 1.50	8.33 ± 0.95	4.69 ± 1.18	164.307	<0.001	HS
Range	1.46 – 2.05	11.15 – 15.47	6.87 – 9.1	3.18 – 6.24			
Post Hoc analysis by LSD							
P1		P2	P3	P4	P5	P6	
<0.001		<0.001	<0.001	<0.001	<0.001	<0.001	

P-value > 0.05: Non significant; *P-value* < 0.05: Significant; *P-value* < 0.01: Highly significant•: One Way ANOVA test. P1: group I Vs group II; P2: group I Vs group III; P3: Group I Vs group IV; P4: Group II Vs group III; P5: Group II Vs group IV; P6: Group III Vs group IV

Table 4: Statistical results of TGβ, TNF-α, iNOS and MDA levels in rat serum

ELISA		Group I (control)	Group II (BOO-Created)	Group III (Resveratrol treated)	Group IV (Botulinum toxin -treated)	Test value	*P-value*	Sig.
		No. = 7	No. = 7	No. = 7	No. = 7			
TGB biochemistry profile	Mean ± SD Range	4.99 ± 1.31 3.4 – 6.8	69.86 ± 17.10 48.28 – 92.35	14.38 ± 3.57 10.2 – 19.5	11.42 ± 2.94 7.82 – 15.26	80.177•	<0.001	HS
TNF-α	Mean ± SD Range	45.72 ± 6.15 39.5 – 53.44	182.86 ± 24.56 158 – 213.76	91.44 ± 12.30 79 – 106.88	68.44 ± 9.31 59.25 – 80.16	115.177•	<0.001	HS
iNOS biochemistry profile	Mean ± SD Range	16.70 ± 1.22 15.2 – 18.5	33.37 ± 2.28 30.8 – 37	27.59 ± 4.78 22.8 – 35.4	15.03 ± 1.10 13.68 – 16.65	70.295•	<0.001	HS
MDA Biochemistry profile	Mean ± SD Range	32.11 ± 1.09 30.2 – 33.4	128.46 ± 4.38 120.8 – 133.6	64.23 ± 2.19 60.4 – 66.8	48.17 ± 1.64 45.3 – 50.1	1792.574•	<0.001	HS
Post Hoc analysis by LSD								
		P1	P2	P3	P4	P5	P6	
TGB biochemistry profile		<0.001	0.060	0.189	<0.001	<0.001	0.538	
TNF-α		<0.001	<0.001	0.008	<0.001	<0.001	0.008	
iNOS biochemistry profile		<0.001	<0.001	0.271	<0.001	<0.001	<0.001	
MDA Biochemistry profile		<0.001	<0.001	<0.001	<0.001	<0.001	<0.001	

P-value > 0.05: Non significant; *P-value* < 0.05: Significant; *P-value* < 0.01: Highly significant •: One Way ANOVA test. P1: group I Vs group II; P2: group I Vs group III; P3: Group I Vs group IV; P4: Group II Vs group III; P5: Group II Vs group IV; P6: Group III Vs group IV

Table 5: Measurements of thickness of the muscularis propria among different groups

Thickness of muscularis propria (µm)	Group I (control)	Group II (BOO-Created)	Group III (Resveratrol treated)	Group IV (Botulinum toxin -treated)	Test value	*P-value*	Sig.
	No. = 7	No. = 7	No. = 7	No. = 7			
Mean ± SD	2.66 ± 0.46	5.01 ± 0.80	2.54 ± 0.35	2.62 ± 0.54	31.836•	<0.001	HS
Range	2.1 – 3.4	4.05 – 6.5	2.15 – 3	2.01 – 3.6			
Post Hoc analysis by LSD							
P1		P2	P3	P4	P5	P6	
<0.001		0.704	0.888	<0.001	<0.001	0.811	

P-value > 0.05: Non significant; *P-value* < 0.05: Significant; *P-value* < 0.01: Highly significant •: One Way ANOVA test. P1: group I Vs group II; P2: group I Vs group III; P3: Group I Vs group IV; P4: Group II Vs group III; P5: Group II Vs group IV; P6: Group III Vs group IV

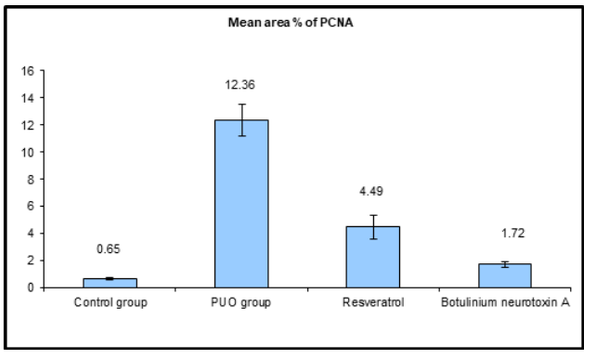

Histogram 1: illustrates area % of PCNA immunoreaction in the muscularis propria

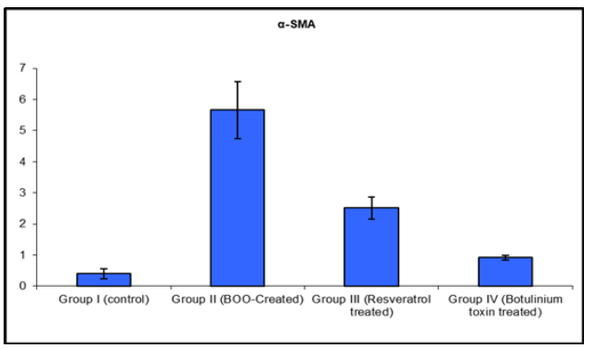

Histogram 2: Mean area % of α-SMA in the muscularis propria of urinary bladder

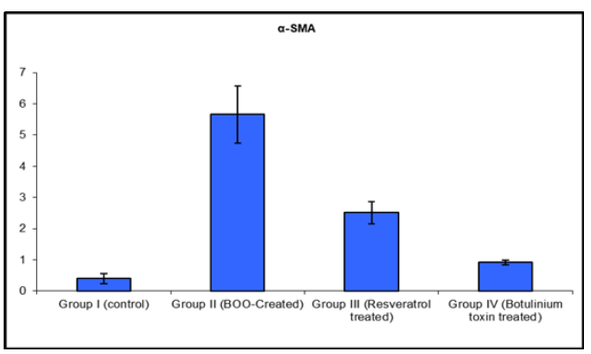

Histogram 3: Mean area % of collagen distribution in the muscularis propria of urinary bladder

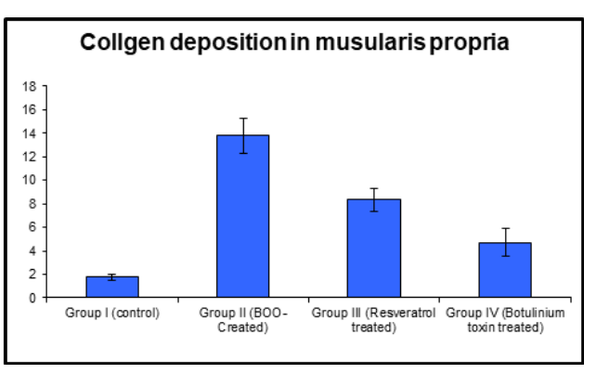

Histogram 4: Statistical results of TGβ, TNF-α, iNOS and MDA levels in rat serum

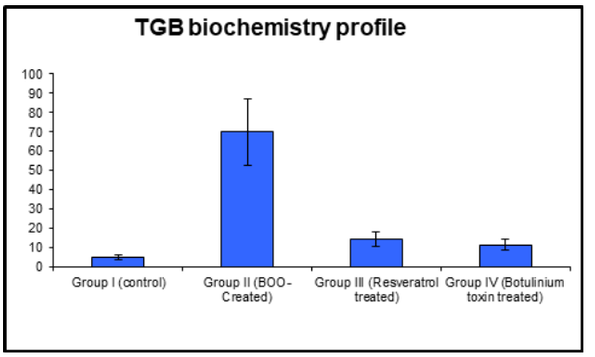

Histogram 5: Estimated rat serum TGB LEVEL

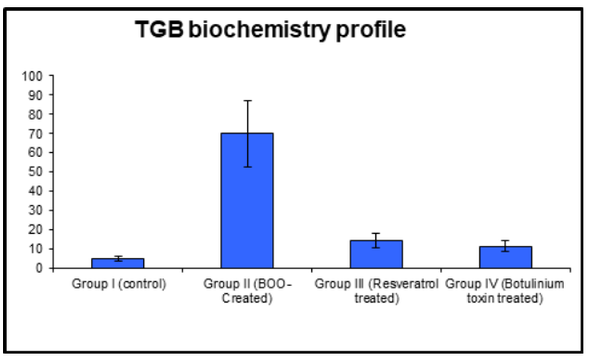

Histogram 6: This is Arepeted Histogram it is the Same as Previous One Delete it

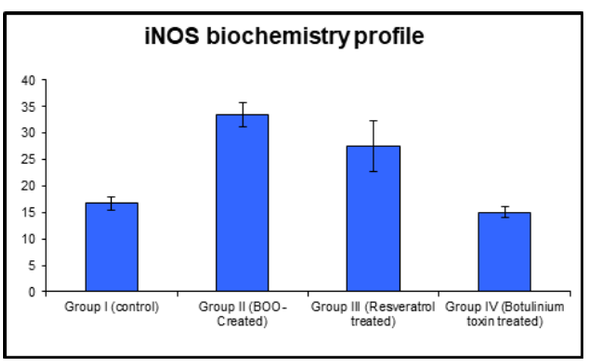

Histogram 7: ESTIMATED RAT SERUM iNOS level

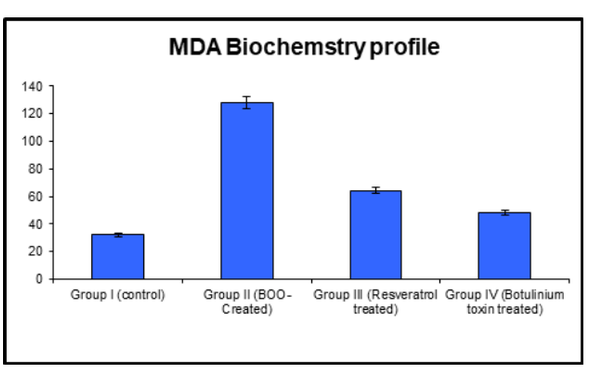

Histogram 8: Estimated rat serum MDA level

DISCUSSION

Partial obstruction of the bladder outlet is a severe urological condition that exposes the bladder to high pressure urine storage and poses a high risk of renal damage. Multiple medications exist for the treatment of OAB[12]. However, antimuscarinic pharmaceuticals currently in use have numerous adverse effects and some patients do not respond adequately to them. Therefore, new and alternative medications must be introduced to the conventional methods of OAB management[7].

Due to their minimal side effects and low prices, natural extracts and medicinal plants receive a great deal of attention. Resveratrol is among the most crucial agents[9]. Resveratrol is a naturally occurring polyphenol found in fruits and vegetation. Recent investigations on humans and animal models have suggested that resveratrol has beneficial properties. In addition, they focused on its ability to enhance metabolic and lipid profiles by virtue of its powerful antioxidant, anti-inflammatory, and anti-proliferative properties. Several urogenital diseases have also been evaluated clinically and experimentally with resveratrol as a therapeutic agent[20]. However, its efficacy in alleviating OAB symptoms and the associated histological and biochemical alterations are still debatable[15].

Alternatively, botulinum neurotoxin A has been utilized in the treatment of lower urinary tract dysfunction (LUTD). It was initially used to treat patients with neurogenic detrusor hyperactivity resulting from a spinal cord injury. Later, Botox was utilized for the treatment of resistant cases of idiopathic detrusor overactivity (IDO) and overactive bladder syndrome. Recently, Botox was authorized for these two clinical conditions. It has been widely utilized to restore urinary continence and enhance the quality of life of patients[3].

In the current investigation the possible role of oral resveratrol versus intramural Botox injection on detrusor muscle hypertrophy, fibrosis and ultrastructural changes was analyzed. Moreover, their potential role on inflammatory markers such as TNFα, TGβ and oxidative stress markers iNOS and MDA levels was also investigated.

In the present work, over active bladder rat model was created by partial urethral obstruction surgery which described previously in details in methods. The muscular bundles appeared markedly disrupted with complete loss to their normal arrangement. In addition to some degenerative changes which were observed in some areas of semithin sections and H&E stained sections. Previous findings could be explained by increased intravesical pressure after PUO and increasing levels of reactive oxygen species production in the urinary bladder wall. This was confirmed by increased serum levels of both MDA and iNOS.

On other hand, increased production of MDA and iNOS already lead to marked change in the metabolic status of detrusor muscle from aerobic to anaerobic state and increased glycogen content in the muscle fibers. This was clearly seen in PAS stained sections of group II. Furthermore, the muscular hypertrophy was clarified by increased immune expression of PCNA in groupII and increased cellular to nuclear ratio which was clearly observed by transmission electron microscopy. Previous studies demonstrated that PCNA expression increased at 24 h after PUO and this increase may reflect cellular hyperplasia and successful model of PUO[5].

In the present study, bladder wall fibrosis was confirmed by Masson's trichrome stain and transmission electron microscopy as there was extensive collagen deposition in between the muscular bundles of muscularis propria. The previous findings may be correlated to increased ROS production and increasing levels of proinflammatory cytokines such as TNFα and TGβ. Moreover, release of inflammatory cells such as mast cells and myofibroblasts also plays a crucial role in increasing the immunoexpression of α-SMA, collagen deposition and tissue fibrosis.

According to prior research, mechanical strain, hydrodynamic pressure and hypoxia are believed to be the pathophysiological causes of PUO[22]. In addition, overactive bladder is typically accompanied by the activation of multiple inflammatory cascades and rising levels of proinflammatory cytokines such as TNF, transforming growth factor beta (TGF-β) and increasing collagen ratios. In human and animal models of PUO, the infiltration of bladder smooth muscle fibers with connective tissue results in the destruction of the bladder's contractile component. Current treatments do not target the inflammation and fibrosis aspects of PUO effectively[18].

On histopathological level, OAB is also associated with an increase in myofibroblasts, which are responsible for aberrant extracellular matrix accumulation and rise in α-smooth muscle actin (α-SMA) expression. Typically, as a consequence of these biochemical alterations, detrusor hypertrophy and instability occur[11].

On other hand, mild to moderate improvement in the histopathological and biochemical profiles was clearly observed in groups III and IV; moderate restoration of normal shape and arrangement of muscle bundles of muscularis propria. Improvement of oxidative stress condition and decreased serum levels of MDA and iNOS. Decreased production of ROS and decreased proinflammatory cytokine levels TNFα and TGβ.Again back to the aerobic metabolic state due to improvement of the condition of the blood vessels and decreased ROS production. The muscle fibers showed negative reaction to PAS stain in both groups III and IV.

Regarding the thickness of muscularis propria; an obvious improvement was observed in group IV. The previous finding could be attributed to decrease of the proliferative potential of the muscle fibers. This was clarified by decreased PCNA immune expression in group III and negative expression in group IV. Marked improvement in the collagen profile was also shown in both groups; but the best was in group IV. In addition

to decreased levels of proinflammatory cytokines TNFα, TGβ and decreased α-SMA immunoexpression. Moreover, the inflammatory cells; mast cells, fibroblasts and myofibroblasts which were detected by transmission electron microscopy became hardly detected.

The present study's findings were consistent with those of He *et al*. (2017)[10], YU *et al*., (2017)[25] and Zeng *et al*., (2018)[26] who established an animal model of chronic prostatitis and investigated the potential role of resveratrol in mitigating symptoms of lower urinary tract dysfunction and highlighted its novel role in symptom relief. Zeng *et al*., (2018)[26] documented the inhibitory effect of resveratrol on the TGFβ-associated profibrotic effects of mast cells. In addition, this study revealed that the number of mast cells and the intensity of their staining were associated with elevated TGFβ production and interstitial fibrosis. Nageib *et al*., (2020) proved that BoNT-A reduced the OAB-associated inflammatory process. This was evident histologically through the reduction of submucosal edema and inflammatory cell infiltrate scores. Moreover, this study proved that BoNT-A can reduce the relative gene expression of proinflammatory cytokines (TGβ and TNF-α) which are increased in the OAB group.

In addition, Nageib *et al*., (2020)[16] measured MDA to determine the antioxidative stress effect of BoNT-A. In the group that received BoNT-A, its concentration decreased significantly according to the results. Furthermore, Watanabe *et al*., (2010)[21] emphasized that intramural BONT-A injection has an inhibitory effect on PCNA expression; therefore, it does not induce cellular proliferation or hyperplasia which is highly consistent with the findings of the present study.

In the current study, some large nerve terminals appeared unaffected by the obstruction due to their thick capsule and independent vascular supply, while others in group II appeared exceedingly dilated and degenerated. In both groups III and IV, there was a noticeable improvement in appearance. In the early phases of obstruction, the nerve terminals at neuromuscular junctions remain unaffected. The injury begins to manifest between 12 and 24 hours after an obstruction. The abnormal-appearing nerve endings, including degenerating endings are observed two days after de-occlusion, but not seven days later. In contrast to the current study, observable alterations were still observed at neuromuscular junctions[8].

CONCLUSION

Results of the present study rendered new lines of management to patients who suffer from over active bladder and its complications. In addition, patients who have refractory symptoms and didn't achieve any improvement on the conventional lines of treatment. The first agent is resveratrol, natural extract, shows minimal or even no adverse effects. In addition to its availability and easy route of administration. Depending upon results of the present work; it may play a fundamental role in minimizing the frequency and urgency and other clinical manifestations of OAB. In addition, it may be used as first line of management as it is given by oral route and it will protect patients from complications of anesthesia and surgical lines of management. The second agent is botulinum neurotoxin A injection. It offered a remarkable improvement in the cytoarchitecture of the urinary bladder and the inflammatory state associated with the OAB. After failure of life style modifications, oral routes such as resveratrol as first lines of management we can conclude with botulinum neurotoxin A injection and other surgical routes of management.

CONFLICT OF INTERESTS

There are no conflicts of interest.

REFRENCES

1. Anggorowati, N., Kurniasari, C.R., Damayanti, K., *et al*., (2017): Histochemical and immunohistochemical study of α-SMA, collagen, and PCNA in epithelial ovarian neoplasm. Asian Pacific journal of cancer prevention: APJCP, 18(3), p.667.
2. Bancroft, J.D &Gamble, M. (2008): Theory and practice of histological techniques. Elsevier health sciences.
3. Barba M, Lazar T, Cola A, *et al*., (2022): Learning Curve of Botulinum Toxin Bladder Injection for the Treatment of Refractory Overactive Bladder. Int. J. Women's Health. 2022 Jan 4; 14:1-7. doi: 10.2147/IJWH.S345454, indexed in PMID: 35018123; PMCID: PMC8742680.
4. Berntsen M, Bøgevig S, Høgberg LCG. *et al*., (2022): Iatrogenic botulism in therapeutic use of botulinum toxin. Ugeskr Laeger. 2022 Feb 14;184(7): V07210574. Danish, indexed in PubMed: 35179113.
5. Chen L, Yang Y, Yang J, *et al*., (2018): Suture causing urethral meatus stricture: A novel animal model of partial bladder outlet obstruction. Neurourology Urodyn. 2018 Sep;37(7):2088-2096. doi: 10.1002/nau.23427. Epub 2018 Jun 28, indexed in PubMed: 29953650.
6. Cox K, Ghebrehiwet M, Kee M, *et al*., (2023): Assessing the Reporting of Harms in Systematic Reviews Focused on the Therapeutic and Cosmetic Uses of Botulinum Toxin. Clinical Drug Investigation 2023 Jan 10. doi: 10.1007/s40261-022-01235-6. Epub ahead of print, indexed in PubMed: 36626045.
7. Dobberfuhl, AD (2022): Pathophysiology, assessment, and treatment of overactive bladder symptoms in patients with interstitial cystitis/bladder pain syndrome. Neurourology. Urodyn. 2022 Nov;41(8):1958-1966. doi: 10.1002/nau.24958. Epub 2022 May 24, indexed in PubMed: 35607890.
8. Gabella G, Uvelius B., (1999): Structural changes in the rat bladder after acute outlet obstruction. Scand J Urol Nephrol Suppl. 1999; 201:32-7. doi: 10.1080/003655999750042123. PMID: 10573774.

9. Gambini, J, Gimeno-Mallench, L, Mas-Bargues, C, *et al*., (2018): Resveratrol in Experimental Models and Humans. In Conn's Handbook of Models for Human Aging (pp. 1143-1156). Academic Press.

10. He Y, Zeng HZ, Yu Y, *et al*., (2017): Resveratrol improves prostate fibrosis during progression of urinary dysfunction in chronic prostatitis. Environ Toxicol. Pharmacol. 2017 Sep; 54:120-124. doi: 10.1016/j.etap.2017.06.025. Epub 2017 Jul, indexed in PubMed: 28704753.

11. Jiang YH, Jhang JF, Lee YK, *et al*., (2022): Low-Energy Shock Wave Plus Intravesical Instillation of Botulinum Toxin A for Interstitial Cystitis/Bladder Pain Syndrome: Pathophysiology and Preliminary Result of a Novel Minimally Invasive Treatment. Biomedicines. 2022 Feb 7;10(2):396. doi: 10.3390/biomedicines10020396, indexed in PubMed: 35203604; PMCID: PMC8962423.

12. Joseph S, Maria SA, and Peedicayil J, (2022): Drugs Currently Undergoing Preclinical or Clinical Trials for the Treatment of Overactive Bladder: A Review. Curr. Ther. Res. Clin. Exp. 2022 Apr 6;96: 100669. doi: 10.1016/j.curtheres.2022.100669, indexed in PubMed: 35494662. PMCID: PMC9052038.

13. Kue, J. (2007): Electron microscopy methods and protocols. New Jersey. Springer. Science & Business Media 3:1-8

14. Liu Q & Liao L, (2022): Nano-BTA: A New Strategy for Intravesical Delivery of Botulinum Toxin A. Int. Neurourology. J. 2022 Jun;26(2):92-101. doi: 10.5213/inj.2142124.062. Epub 2022 Jun 30, indexed in PubMed PMID: 35793987; PMCID: PMC9260331.

15. Mitsunari K, Miyata Y, Matsuo T, *et al*., (2021): Pharmacological Effects and Potential Clinical Usefulness of Polyphenols in Benign Prostatic Hyperplasia. Molecules. 2021 Jan 16;26(2):450. doi: 10.3390/molecules26020450, indexed in PubMed: 33467066; PMCID: PMC7829696.

16. Nageib M, Zahran MH, El-Hefnawy AS, *et al*., (2020): Low energy shock wave-delivered intravesical botulinum neurotoxin-A potentiates antioxidant genes and inhibits proinflammatory cytokines in rat model of overactive bladder. Neurourology Urodyn. 2020 Nov;39(8):2447-2454. doi: 10.1002/nau.24511. Epub 2020 Sep 22, indexed in PubMed: 32960981.

17. Peyronnet B, Mironska E, Chapple C, *et al*., (2019): A Comprehensive Review of Overactive Bladder Pathophysiology: On the Way to Tailored Treatment. Eur. Urol. 2019 Jun;75(6):988-1000. doi: 10.1016/j.eururo.2019.02.038. Epub 2019 Mar 26, indexed in PubMed: 30922690.

18. Prata C, Maraldi T, Angeloni C. (2022): Strategies to Counteract Oxidative Stress and Inflammation in Chronic-Degenerative Diseases. Int. J Mol. Sci. 2022 Jun 9;23(12):6439. doi: 10.3390/ijms23126439, indexed in PubMed PMID: 35742882; PMCID: PMC9223535.

19. Robertson I, Wai Hau T, Sami F. *et al*., (2022): The science of resveratrol, formulation, pharmacokinetic barriers and its chemotherapeutic potential. Int. J Pharm. 2022 Apr 25;618: 121605. doi: 10.1016/j.ijpharm.2022.121605. Epub 2022 Feb 26, indexed in PubMed: 35227804.

20. Vicari E, Arancio A, Catania VE, *et al*., (2020): Resveratrol reduces inflammation-related Prostate Fibrosis. Int. J. Med Sci. 2020 Jul 19;17(13):1864-1870. doi: 10.7150/ijms.44443, indexed in PubMed: 32788865; PMCID: PMC7415386.

21. Watanabe T, Masago T, Miyagawa I. (2010): Apoptotic action of botulinum toxin on detrusor muscle in rats. Urol. Int. 2010;84(3):341-6. doi: 10.1159/000288240. Epub 2010 Apr 13, indexed in PubMed PMID: 20389167.

22. Wiafe B, Adesida A, Churchill T, *et al*., (2017): Hypoxia-increased expression of genes involved in inflammation, dedifferentiation, pro-fibrosis, and extracellular matrix remodeling of human bladder smooth muscle cells. In *Vitro* Cell Dev Biol. Anim. 2017 Jan;53(1):58-66. doi: 10.1007/s11626-016-0085-2, indexed in PubMed Epub 2016 Sep 8. PMID: 27632054.

23. Wu YH, Chueh KS, Chuang SM. *et al*., (2021): Bladder Hyperactivity Induced by Oxidative Stress and Bladder Ischemia: A Review of Treatment Strategies with Antioxidants. Int. J. of Mol. Sci. 2021 Jun 2;22(11):6014. doi: 10.3390/ijms22116014, indexed in PubMed: 34199527; PMCID: PMC8199707.

24. Yilmaz-Oral D, Kaya-Sezginer E, Asker H, *et al*., (2022): Co-administration of sodium hydrosulfide and tadalafil modulates hypoxia and oxidative stress on bladder dysfunction in a rat model of bladder outlet obstruction. Int. Braz. J. Urol. 2022 Nov-Dec;48(6):971-980. doi: 10.1590/S1677-5538.IBJU.2022.0207, indexed in PubMed PMID: 36173409; PMCID: PMC9747034.

25. Yu Y, Jiang J, He Y, *et al*., (2017): Resveratrol improves urinary dysfunction in rats with chronic prostatitis and suppresses the activity of the stem cell factor/c-Kit signaling pathway. Mol Med Rep. 2017 Aug;16(2):1395-1400. doi: 10.3892/mmr.2017.6721. Epub 2017 Jun 8, indexed in PubMed PMID: 29067468.

26. Zeng H, He Y, Yu Y, *et al*., (2018): Resveratrol improves prostate fibrosis during progression of urinary dysfunction in chronic prostatitis by mast cell suppression. Mol. Med. Rep.17(1): p.918–924. doi: 10.3892/mmr.2017.7960.

الملخص العربى

التأثير المحتمل لحقن سم البوتولينوم العصبي من النوع أ داخل جدار المثانه مقابل الريسفيراترول الفموي علي تقليل التضخم والتليف والتغيرات الهيكلية للعضلة النافصة التي تحدث بشكل ثانوي لانسداد مجرى البول الجزئي في نموذج فئران لمثانه مفرطة النشاط و منظور حول تأثيرهما على TNFα, TGβ, PCNA و α-SMAوiNOS

ولاء عادل عبد المعز

قسم التشريح والأجنة، كلية الطب، جامعة عين شمس، مصر

المقدمة: تؤثر الحالة السريرية لفرط نشاط المثانة على مليارات الأفراد. ويعد السبب الأكثر شيوعًا هو النشاط المفرط للعضلات النافصه في جدار المثانه البوليه.لذلك يجب تزويد المرضى الذين تكون أعراضهم مقاومة للعلاج التقليدي بخيارات علاجية جديدة.لذلك كان الهدف من الدراسه الحاليه تقييم تأثير حقن البوتولينوم العصبي A مقارنة بالريسفيراترول الفموي على التغيرات النسيجية المرضية التي تحدث بشكل ثانوي لانسداد مجرى البول الجزئي وتقييم تأثيرها على TNFα و TGβ و PCNA و α-SMA و iNOS.

٤٠ جرذًا بالغًا تم تضمينهم في الدراسة. المجموعة الأولى (مجموعة الشام). المجموعه الثانيه: تم إنشاء نموذج انسداد مجرى البول الجزئي وترك الفئران لمدة ٦ أسابيع. المجموعة الثالثة: ١٠ مجم / كجم ريسفيراترول يعطى عن طريق الفم لمدة أسبوعين (من الاسبوع السادس بعد اجراء الانسداد الجزئي للمجري البولي للجرذان حتى نهاية الأسبوع الثامن). المجموعة الرابعة: بعد اجراء العمليه لهذه المجموعه، تم حقن ٥٠ مل من البوتولينوم العصبي في جدران مختلفة من المثانة. تم ترك الفئران لمدة أسبوعين آخرين ثم تم التضحية بها.

النتائج: أظهرت المجموعة الثانية حزم عضلية متقطعة من البروبريا العضلية. ظهرت ألياف العضلات مع فجوات حشوية واسعة وشكل غير طبيعي لنواتها. أظهرت مقاطع ثلاثية الألوان من ماسون ترسبًا واسعًا للكولاجين في جدار المثانة. رد فعل مكثف على PAS وصبغ عميق لألياف العضلات. أظهر المجهر الإلكتروني النافذ حدودًا خلوية غير منتظمة وشكلًا غريبًا لغشاء الخلية. ظهرت الأورمات الليفية العضلية على نطاق واسع وهي تغزو الحاجز العضلي. بدت بعض ألياف العضلات متدهورة نتيجة تسلل واسع النطاق من الخلايا البدينة والأورمات الليفية. إلى جانب ذلك ، نهايات عصبية متوسعة للغاية مع أجسام متدهورة متجمعة في نهاياتها السفلية. يمكن أيضًا اكتشاف الأوعية الدموية المتوسعة والمحتقنة. كانت هناك زيادة ملحوظة في علامات الإجهاد التأكسدي والسيتوكينات المنشطة للالتهابات. تحسنت جميع التغييرات السابقة بشكل كبير في المجموعتين الثالثة والرابعة ولوحظت أفضل النتائج في المجموعة الرابعة.

الخلاصة: المستخلص من الدراسه هو ريسفيراترول وسم عصبي البوتولينوم هما خطان جديدان للإدارة للمرضى الذين يعانون من أعراض مقاومة فرط نشاط المثانة.